

Chapter 5 – FIBER-PUMPED FREQUENCY CONVERSION DEVICES

5.1 BACKGROUND AND PREVIOUS WORK

Contributors to this section: Christelle Kieleck¹, Antoine Berrou¹, Marc Eichhorn¹; Francis Théberge², Pierre Mathieu², Denis Vincent², Jean-François Daigle³, Alain Villeneuve⁴, Joseph Salhany⁴, Brian Burgoyne⁴, Yasaman Soudagar⁴, Marc Châteauneuf², Jacques Dubois², Rita D. Peterson⁵

Mid-IR lasers find interesting applications in medicine, remote sensing [1], molecular spectroscopy of pollutants [2], detection of threats [3], etc. Ideally, the ultimate mid-IR laser should be intrinsically robust to mechanical vibrations, stable over temperature fluctuations, tunable over a broad spectral range, and efficient for low power consumption. A technology that could meet all these goals is the mid-IR fiber laser. Efficient and tunable rare-earth-doped mid-IR fiber lasers do not exist yet, and they still require the development of single-mode Infrared (IR) fibers and highly efficient pump sources [4]. Chalcogenide, fluoride and telluride fibers are under development to access spectral bands beyond the capability of silica, both as laser hosts and as non-linear materials. Fiber laser and mid-infrared supercontinuum generation studies are in progress. Substantial improvements in areas such as loss, power/energy handling, and active ion incorporation must occur, however, to allow for an all-fiber solution in the mid-IR.

An intermediate step toward completely fiber-based sources is a mid-IR source based on fiber-pumped frequency converters. The most mature and readily available fiber pump sources emitting in the near-infrared are Tm³⁺- and Ho³⁺-doped fibers operating around 2 μm . These are available as commercial products that are relatively robust, compact, efficient, and high in power and energy. In addition, their output is already farther in the infrared than that of more common Yb-based fibers. However, 2 μm fiber technology still suffers from a lack of commercial fiber components for high power and high energy operation – even though some fiber components are emerging [5].

On the non-linear material side, only a few crystals can fulfill the wavelength requirements associated with high-power applications in the atmospheric windows (3 – 5 μm and 8 – 12 μm): PPLN, covering only part of the 3 – 5 μm region; ZnGeP₂ (ZGP); and Orientation-Patterned Gallium Arsenide (OPGaAs). The website of Inrad, a vendor of ZGP, already claims that “recent advances in 2 μm fiber laser technology have increased the potential of ZGP for use in ruggedized, compact optical set-ups. Pumping ZGP with a fiber laser instead of a solid-state source could substantially reduce the footprint of the entire system (IRCM System)” [6]. Unfortunately ZGP and OPGaAs crystals are still not readily available, and other emerging non-linear crystals, though promising, remain untested.

Up to now, Optical Parametric Oscillators (OPO) that could generate mid-IR laser radiation have been developed, but these OPOs can generate only a few wavelengths at a time. Moreover these OPOs are sensitive to mechanical vibrations and temperature fluctuations, and thus difficult to implement for real applications in the field. Another high-potential mid-IR laser source under development is the Quantum Cascade Laser (QCL) which is based on microstructured semi-conductors usually requiring low-temperature cooling for achieving high power output. QCLs are however, not tunable over a broad spectral range, and thus several QCLs are needed in parallel to cover some specific wavelengths in the mid-IR spectral region [7].

¹ ISL, French-German Research Institute of Saint-Louis, 5 rue du Général Cassagnou, 68300 Saint-Louis Cedex, France.

² DRDC Valcartier, 2459 route de la Bravoure, Québec (Québec) G3J 1X5, Canada.

³ AEREX Avionics Inc., 324 St-Augustin Avenue, Breakeyville (Québec) G0S 1E1, Canada.

⁴ Genia Photonics Inc., 500 Cartier Blvd. West, Suite 131, Laval (Québec) H7V 5B7, Canada.

⁵ Air Force Research Laboratory, AFRL/RYPDH Bldg 620, 2241 Avionics Circle, Wright-Patterson AFB, OH 45433, United States.

FIBER-PUMPED FREQUENCY CONVERSION DEVICES

This chapter will give part of the state-of-the-art of non-linear converters directly pumped by a fiber laser, and will concentrate only on those devoted to 3 – 5 μm emission, especially for DIRCM applications.

5.2 EXPERIMENTAL RESULTS

5.2.1 PPLN-Based Systems

Periodically Poled Lithium Niobate (PPLN) is a mature and widely available commercial non-linear crystal that can readily be directly fiber-pumped. As it is limited by intrinsic absorption to a maximum operating wavelength of approximately 4 μm , complete wavelength coverage for DIRCM application is not possible with this material system. As an example, set-ups are briefly described which can deliver average power in excess of 1 W in the 3.8 – 4.0 μm wavelength range at a pulse repetition frequency of 100 kHz and an average power of 0.25 W at 4.5 μm wavelength. The original design and performance of tunable mid-IR generation by fiber-pumped difference frequency mixing in PPLN, undertaken at DRDC, Canada, is described in detail.

5.2.1.1 Singly Resonant PPLN OPO Pumped by an Adjustable PRF 100 kHz, Linearly Polarized, 1545 nm Wavelength Pulsed Fiber Source

A mid-IR source consisting of a 10 W average-power, linearly polarized 1.54 μm wavelength pulsed fiber source pumping an optical parametric oscillator was reported, (Figure 5-1) [3]. From this source, average power in excess of 1 W in the 3.8 – 4.0 μm wavelength range at a pulse repetition frequency of 100 kHz was obtained. With a slightly different set-up, an average power of 0.25 W at 4.5 μm wavelength was achieved. Components are bulk with free-space coupling.

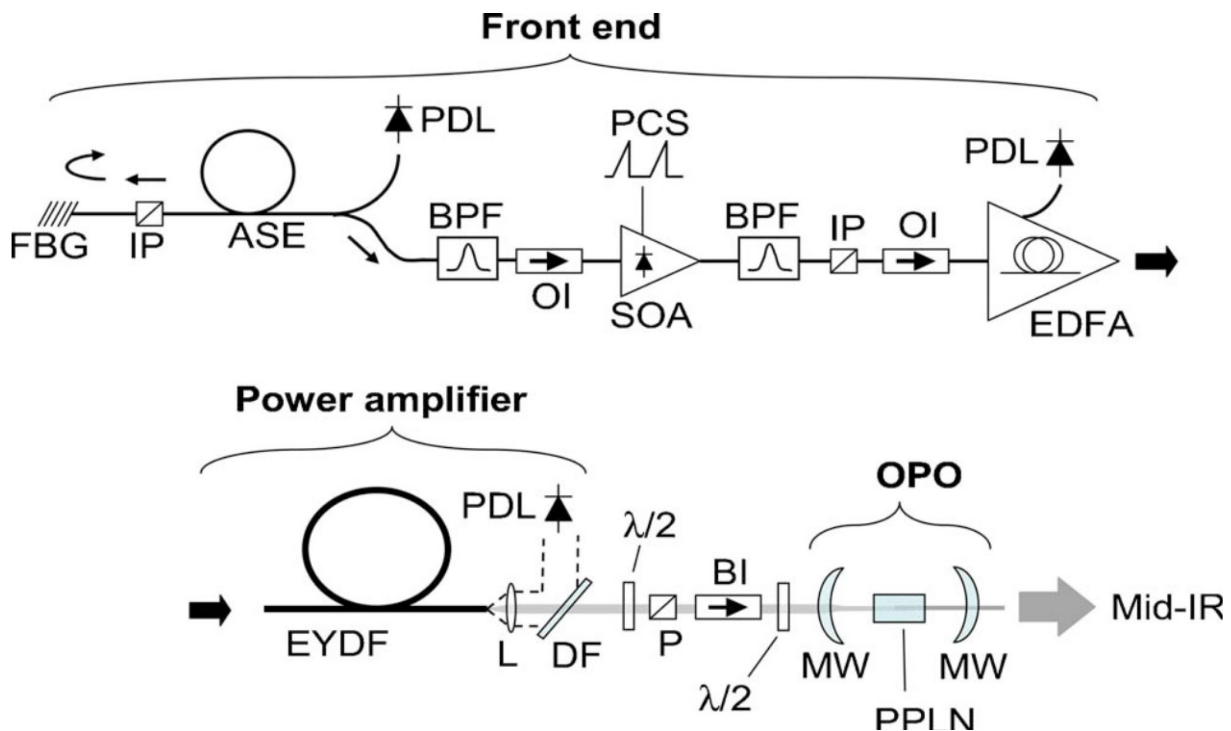


Figure 5-1: Layout of Mid-IR Source: Singly Resonant PPLN OPO Pumped by an Adjustable PRF 100 kHz, Linearly Polarized, 1545 nm Wavelength Pulsed Fiber Source.

5.2.1.2 Tunable Mid-Infrared Generation by Fiber-Pumped DFM in PPLN

Contributors to this section: Francis Th  berge⁶, Jean-Fran  ois Daigle⁷, Alain Villeneuve⁸, Joseph Salhany⁸, Brian Burgoyne⁸, Yasaman Soudagar⁸, Marc Ch  teauneuf⁶, Jacques Dubois⁶

We present here a design based on Difference-Frequency Generation (DFG) in a non-linear crystal pumped by synchronized and tunable commercially available Near-Infrared (NIR) fiber lasers. This idea is not new and has been explored by others groups [8]-[12], but the latest innovations in NIR fiber lasers [13] have enabled the creation of fast-scanning picosecond fiber lasers.

The key element for the generation of a fast tunable mid-IR laser source through DFG is the programmable Erbium-doped fiber laser which combines dispersive elements with a synchronized Electro-Optic Modulator (EOM). This first fiber laser can emit any wavelength within the gain band, quickly tune to any wavelength in this range, and program any spectrally encoded signal. The basis of this laser is schematically presented in Figure 5-2(a). With an Erbium-doped fiber used as gain medium, a Wavelength Division Multiplexer (WDM) couples the energy of a 980 nm laser diode to provide core pumping. An Optical Coupler (OC) extracts a portion of the amplified light and delivers it to the next stage (Figure 5-3). The Programmable Laser (PL) is dispersion-tuned. A series of three Chirped Fiber Bragg Gratings (CFBG) serve as the dispersive element for covering as much of the Erbium-gain spectrum as possible, and are addressed by a circulator. The timing of the pulses to the EOM then determines which wavelength will see amplification by coordinating activation of the EOM with the arrival of the desired wavelength's pulse wavefront.

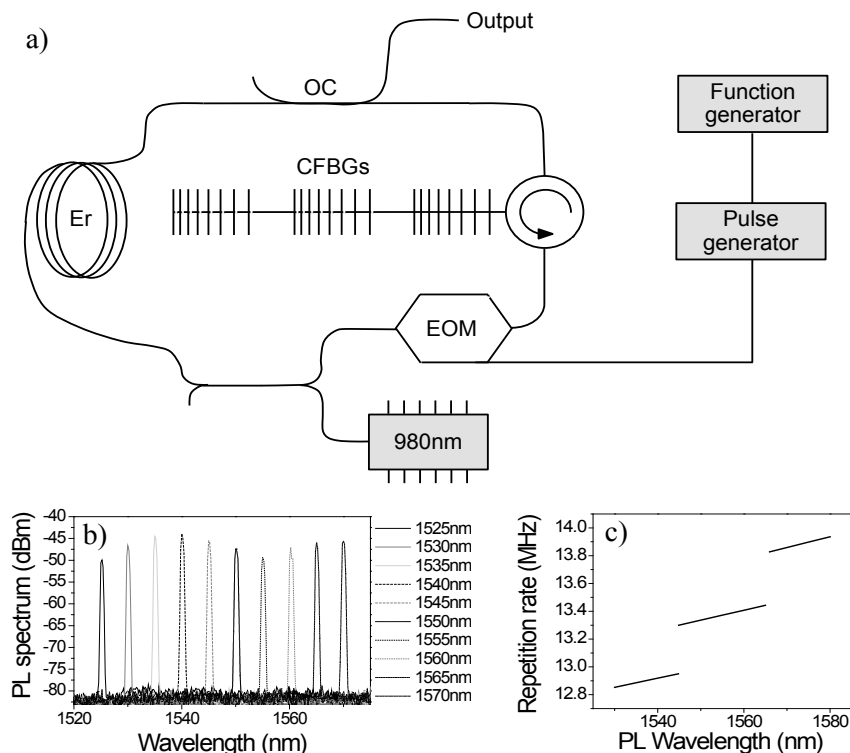


Figure 5-2: (a) Schematic of the Programmable Erbium-Doped Fiber Laser, Including: Electro-Optic Modulator (EOM), Output Coupler (OC), Chirped Fiber Bragg Grating (CFBG), Wavelength Division Multiplexer (WDM); (b) Samples of Laser Output Spectrum; (c) Repetition Rate as a Function of Amplified Wavelength.

⁶ DRDC Valcarter, 2459 route de la Bravoure, Qu  bec (Qu  bec) G3J 1X5, Canada.

⁷ AEREX Avionics Inc., 324 St-Augustin Avenue, Breakeyville (Qu  bec) G0S 1E1, Canada.

⁸ Genia Photonics Inc., 500 Cartier Blvd. West, Suite 131, Laval (Qu  bec) H7V 5B7, Canada.

FIBER-PUMPED FREQUENCY CONVERSION DEVICES

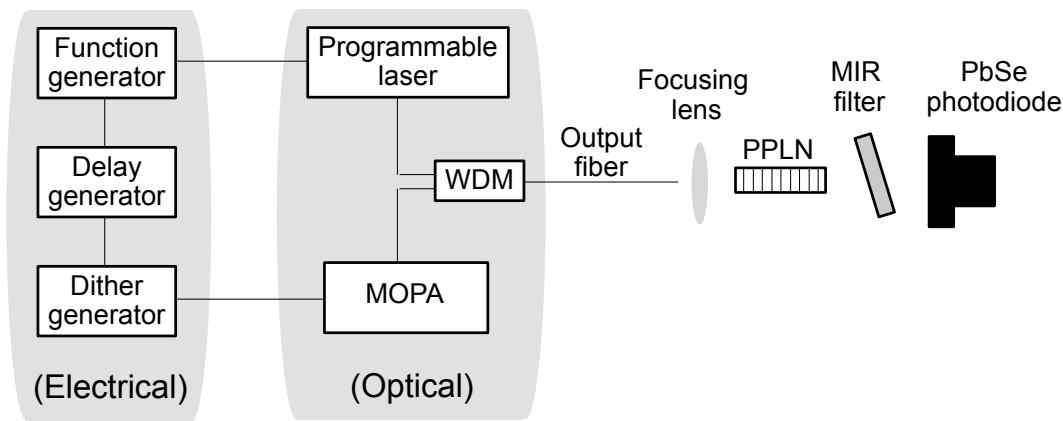


Figure 5-3: Set-Up for Generation and Characterization of the Tunable Mid-IR Laser. The programmable laser and MOPA outputs are combined by a broadband WDM. Both lasers are synchronized and controlled by high-speed electronics driven by software. At the output end of the fiber, the combined beams are focused into the PPLN crystal. The mid-IR output is filtered and its power measured by the PbSe photodiode.

Because of the small distance between the three CFBGs in this system, we observe two jumps in Figure 5-2(c), the graph of repetition rate as a function of wavelength. In fact, the signal applied to the EOM controls four parameters:

- Wavelength;
- Wavelength sweep;
- Repetition rate; and
- Optical pulsewidth.

The EOM is driven by a function generator/pulse generator combination. Operated on its own, the PL can output more than 10 million different optical frequencies per second with very high accuracy, stability, and reproducibility. Since the PL is a dispersion-tuned actively mode-locked laser, wavelengths may be selected in any arbitrary order, enabling wavelength sweeps in either sequential or arbitrary wavelength sequences. Wavelengths can be selected from the entire range or a partial range. The steps between adjacent wavelengths may be arbitrary or may be defined through the user interface in any arbitrary order.

In order to generate mid-IR signal through DFG, we needed an Ytterbium-doped fiber laser synchronized with the Erbium-based PL. One such picosecond laser system is the Synchronized Programmable Laser (SPL) from Genia Photonics that combines these two picosecond fiber laser systems in which both output pulses are synchronized at the DFG crystal (Figure 5-3). The SPL system used for these works consists of the Erbium-doped PL combined with an Ytterbium-doped fiber-based Master Oscillator Power Amplifier (MOPA). A WDM combines the two laser outputs into a single beam. The PL and MOPA use high-speed electronics to drive their internal EOM with precisely timed picosecond pulses.

The synchronization lies within a novel low-jitter function generator circuit capable of generating multiple signals to trigger the pulse generators of each laser. These signals can compensate for any delay in the external optical set-up, ensuring that pulses from both lasers are synchronized at the DFG crystal. Because the 9 μm core output fiber guides both laser beams, spatial overlap is automatically achieved and maintained up to the DFG crystal without the need for any alignment. The laser beams are focused into a 25-mm long PPLN crystal in single pass geometry. For the DFG scheme, the Ytterbium laser corresponds to the pump and the tunable Erbium laser is the signal, with the frequency of the mid-IR output given by the difference of frequency between the pump and the signal. After the PPLN crystal, residual pump and signal from the NIR lasers are filtered out by an AR-coated Germanium window. A calibrated PbSe photodiode is used to measure the power of the generated mid-IR beam.

The PL was continuously tunable from 1525 nm to 1600 nm while the wavelength of the MOPA was fixed at 1080 nm. In principle, the DFG could produce a mid-IR source tunable from 3.32 – 3.7 μm . However the temperature control of the PPLN oven limited the phase-matching such that tunability was possible only from 3.52 – 3.57 μm , with a quantum efficiency of 44% (Figure 5-4(a)). For a 25-mm long PPLN crystal with a grating period of 29.6 μm , the DFG phase-matching bandwidth for a fixed temperature was 2.6 nm, broad enough for our 25 ps pulse train having a spectral width of 0.25 nm.

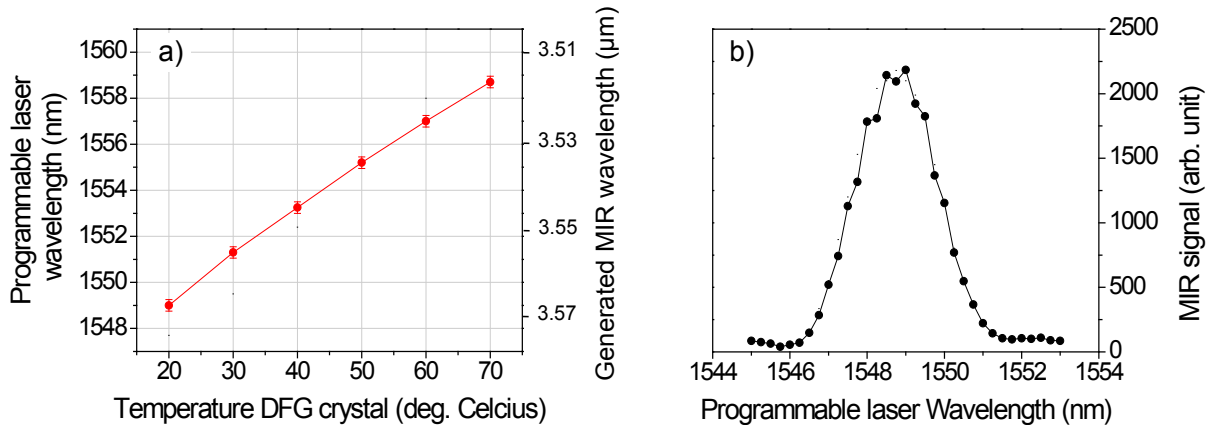


Figure 5-4: Measured DFG Phase-Matching in the PPLN Crystal as a Function of the Temperature (a) and DFG Phase-Matching Window of the PPLN (25 mm long) at Temperature of 20°C (b).

In order to exploit the entire spectral range of the PL, we used two other PPLN crystals with periods of 29.5 μm and 29.7 μm . Figure 5-5(a) presents examples of mid-IR spectra generated using the SPL at the maximum power for both the PL (35 mW) and the MOPA (32 mW). These spectra were measured with a grating-based monochromator and a Mercury Cadmium Telluride detector, and were obtained at the optimum delay between the PL and the MOPA pulses to produce maximum mid-IR output power. In these cases, we could almost cover the entire spectral range of the PL and an efficient mid-IR output was obtained from 3.4 – 3.7 μm . The double-peak structure observed in each spectrum is due to the Self-Phase Modulation (SPM) of the PL pulse occurring in the 2-m long fiber used to transport the output of the WDM to the PPLN crystal.

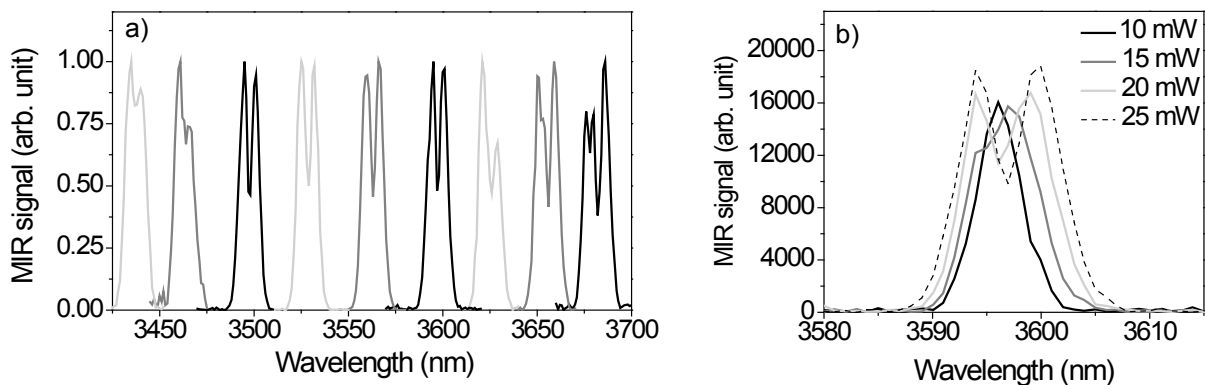


Figure 5-5: Normalized Mid-IR Spectrum Measured for Different PL Wavelengths, and PPLN Crystals with Periods of 29.7 μm and 29.5 μm (a); Mid-IR Spectrum Centred at 3.6 μm as a Function of PL Power (b).

FIBER-PUMPED FREQUENCY CONVERSION DEVICES

Figure 5-5(b) illustrates the impact of the SPM by showing the spectral distribution of the mid-IR beam generated at 3.6 μm as a function of the PL power. At low power (10 mW), we observe a near-Gaussian spectral profile for the generated mid-IR beam. As the PL power was increased, spectral broadening was observed and then the double-peak structure became more pronounced. It is important to note that similar spectral broadening was evidently observed for the PL pulse at the output fiber (before the PPLN), but no spectral broadening was observed for both the PL and MOPA before the output fiber (i.e. after the WDM) at their maximum power. These observations clearly point to the 2-m long output fiber as the origin of the SPM. The use of a shorter fiber, or simply bypassing such fiber will definitely minimize the SPM.

Figure 5-6 shows the linear relationship between the mid-IR output power and the MOPA power injected into the PPLN crystal. The FWHM for the laser beam focused inside the PPLN was around 35 μm , which corresponds to a peak power density of 9 MW/cm^2 at the maximum injected power. Interestingly, by preserving the same power density in the PPLN, we could scale up the pump to 5 watts by focusing it to a diameter of 440 μm in the PPLN. Finally, by preserving a similar quantum efficiency of 44%, we could expect the generation of more than 100 mW of mid-IR output around 3.6 μm wavelength.

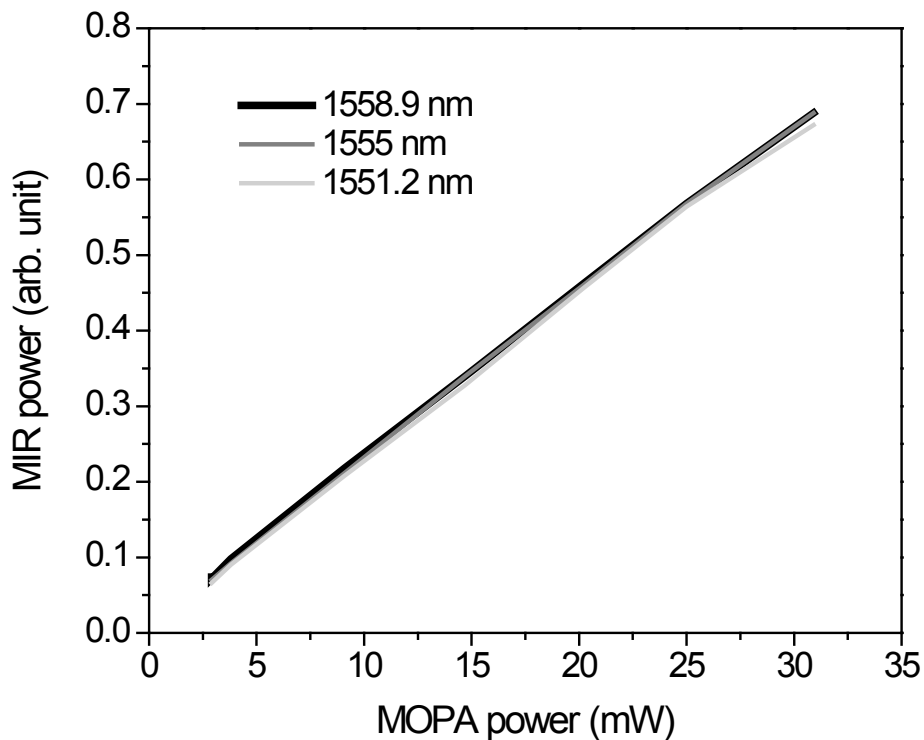


Figure 5-6: Mid-IR Power as a Function of MOPA Power. The PL power was maintained at its maximum for these measures.

The tunability of the mid-IR laser source as presented here was limited by the temperature control for the phase matching, but use of a chirped PPLN crystal would allow much wider tunability and very fast wavelength scanning at a fixed crystal temperature. Such a chirped PPLN crystal could be very long, given that the current 25-mm long PPLN crystal had a QPM bandwidth 10 times larger than the spectral bandwidth of the picosecond laser used in the experiment. By choosing the appropriate wavelengths for the PL and the MOPA, the DFG can be tuned over a wide range of operating wavelengths. For example, by using a tunable PL between 1020 nm and 1110 nm and a tunable MOPA between 1525 nm and 1605 nm the DFG idler can be tuned between 2.8 μm and 4.1 μm . It is also possible to increase by few orders of magnitude the laser powers injected into the chirped PPLN crystal, and consequently, to increase proportionally the mid-IR

output power by using a larger mode area fiber, longer pulsewidth for the SPL, and a shorter transport fiber before the PPLN crystal.

5.2.2 ZnGeP₂-Based Systems

ZGP is currently the most mature mid-IR non-linear crystal, offering efficient non-linear conversion in the mid- and long-wave-IR for countermeasures and other applications. ZGP OPOs pumped by Q-switched solid-state Ho:YAG lasers operating in the 2 μm spectral region have demonstrated very impressive results. Progress in fiber and fiber laser development has led to an increase in output power achievable from pulsed fiber systems. The high peak power and near diffraction-limited beam quality of these fibers make them an ideal source for driving non-linear frequency conversion in ZGP.

Daniel Creeden and co-workers reported the first mid-IR ZGP OPO pumped by a pulsed Tm-doped fiber laser [14],[15]. The fiber pump laser is a Master-Oscillator/Fiber-Amplifier (MOFA) configuration (Figure 5-7). The seed signal is generated by gain-switching a Tm-doped fiber, which produces 30 ns pulses at 1.995 μm at 100 kHz repetition rate. These pulses are amplified in a dual-stage Tm-Doped Fiber Amplifier (TDFA) chain. At the output of the TDFA's, the seed has been amplified more than 24 dB to 21 W of average output power (30 ns pulses, 100 kHz PRF) in a near-diffraction-limited beam with an M^2 of 1.1 ± 0.05 (Figure 5-8(a)). An optical isolator is placed in-line after the amplifiers to prevent feedback and to polarize the beam. Only 60% of the power is transmitted by the isolator, leaving 12.7 W of linearly polarized 1.995 μm light to pump the OPO, enough to produce 2 W of output power in the mid-IR in the 3.4 – 3.9 μm and 4.1 – 4.7 μm spectral regions simultaneously (Figure 5-8(b)).

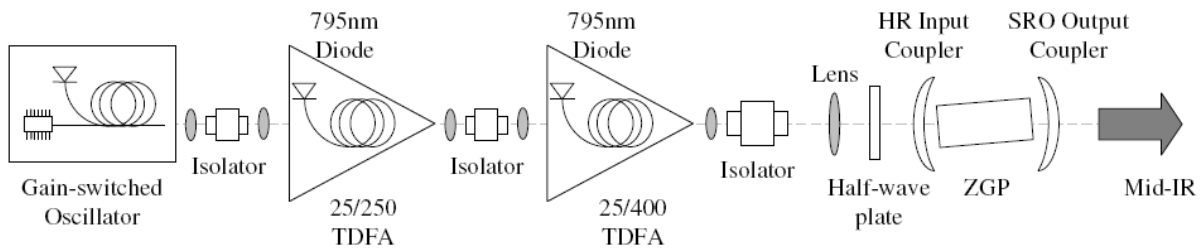


Figure 5-7: Schematic of the Tm-Fiber Amplifier Chain and ZGP Mid-IR OPO.

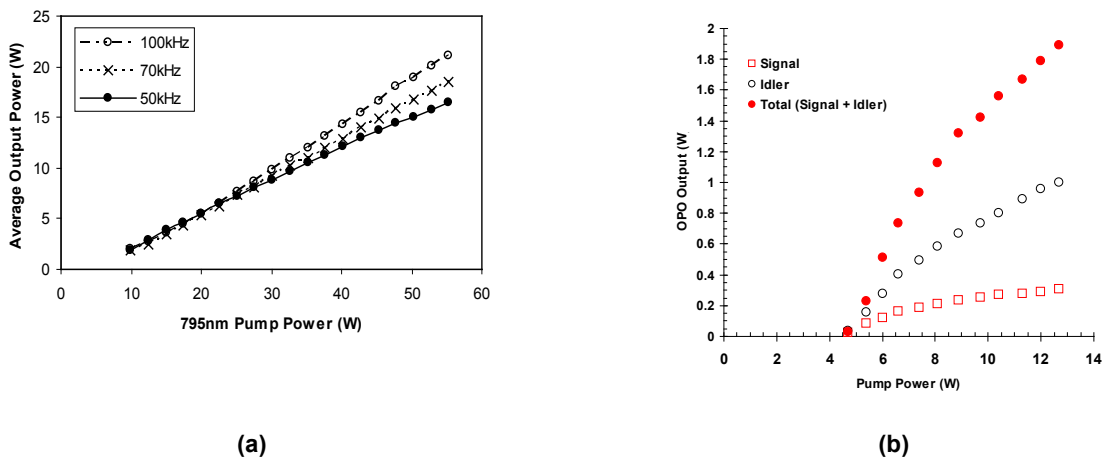


Figure 5-8: Tm-Doped Fiber Amplifier (TDFA) Average Output Power vs. Pump Power (a) and ZGP OPO Output vs. 2 μm Pump Power (b).

FIBER-PUMPED FREQUENCY CONVERSION DEVICES

The authors claimed that the set-up was not optimized, and suggested that future work focus on reducing the OPO threshold and improving conversion efficiency by power scaling the pump and reducing the oscillator pulse width such that a larger pump spot may be used to produce a high optical intensity in the ZGP. These changes could reduce walk-off, increase the interaction length in the crystal, and reduce the thermal lensing, thus decreasing the OPO threshold and improving conversion. They also mentioned that they have planned to examine various cavity configurations and the use of engineered materials, such as orientation-patterned GaAs, as ways to improve conversion efficiency.

A workshop on Mid-Infrared Fiber Lasers (NATO SET-171) was organized at the French-German Research Institute of Saint-Louis (ISL) on 28-29 September 2010 [16]. At the workshop, Daniel Creeden presented an overview of considerations for rare-earth-doped fibers used in pumping non-linear frequency conversion devices. He suggested that efforts should concentrate on promising Tm and Tm:Ho fiber development, because of their high efficiency and wavelength advantages. He also emphasized the need to develop fibers and components especially to eliminate free-space coupling in future fiber systems, allowing systems that are completely optically confined.

Since 2010 efforts in industry have concentrated on the development of fibers based on Tm and Ho, and on fiber components for the 2 μm wavelength range, and research groups have published mid-IR ZGP OPO results obtained using a pulsed Tm-doped fiber laser.

Australia's Defence Science and Technology Organisation reported highly efficient 2 μm fiber lasers based on Tm- and Ho-doped fibers, and reported the use of a 2 μm fiber source for parametric generation of mid-IR output in ZGP [17]. In this experiment, a pulsed master oscillator generated low energy pulses at a high repetition rate: 60 μJ pulses, 50-ns long at 150 kHz prf. (Figure 5-9, Figure 5-10 and Figure 5-11). These were then amplified in a Large-Mode-Area (LMA) Tm-Doped Fiber (TDF) with a 25-μm diameter core, producing 300 μJ pulses at a wavelength of 2050 nm. The output of the amplifier was then focused into an OPO cavity containing a 16-mm ZGP crystal. The cavity consisted of mirrors with a 200 mm radius of curvature, separated by 20 mm, with 10% outcoupling at 3.5 – 5 μm. The publication claimed that optical parametric oscillation was achieved but without giving performance data. In this fiber pump set-up (master oscillator and fiber amplifier), most of the components were still bulk components with free space coupling.

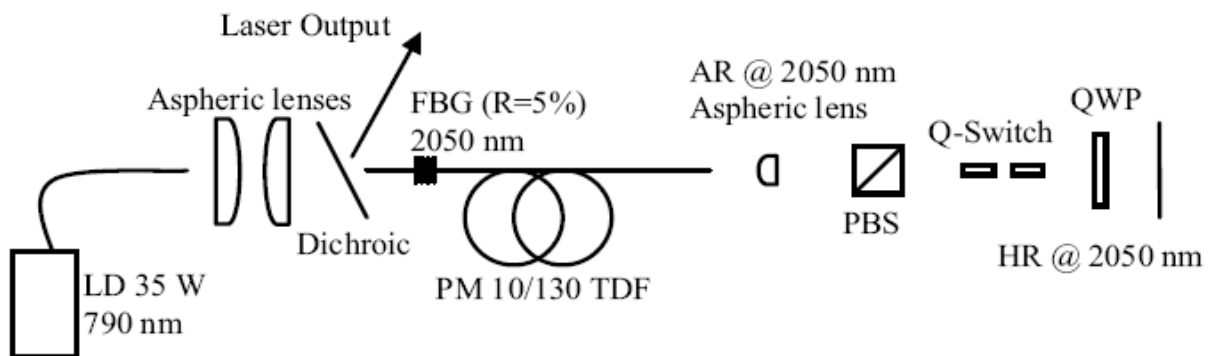


Figure 5-9: Schematic of Electro-Optically Q-Switched Master Laser.

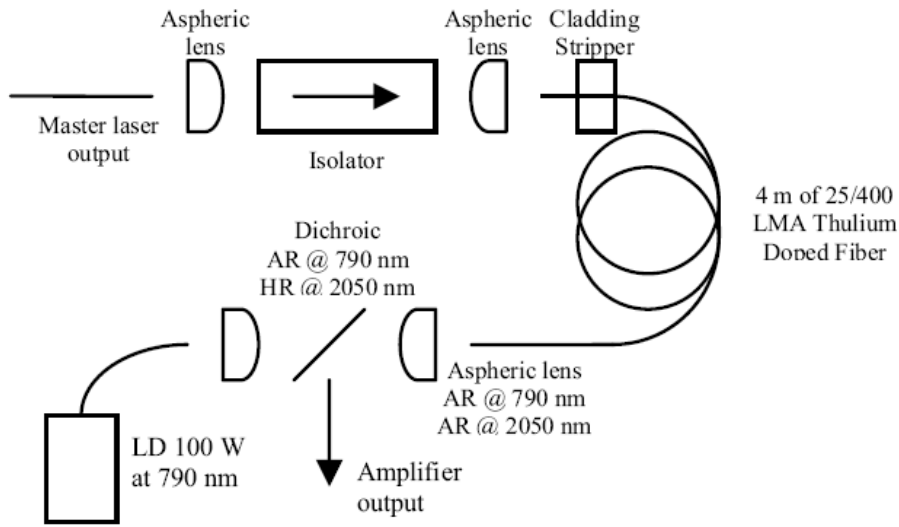


Figure 5-10: The Output of the Master Laser is Propagated Through an Isolator and Coupled into the Core of the Amplifier. The amplifier is pumped from the output end.

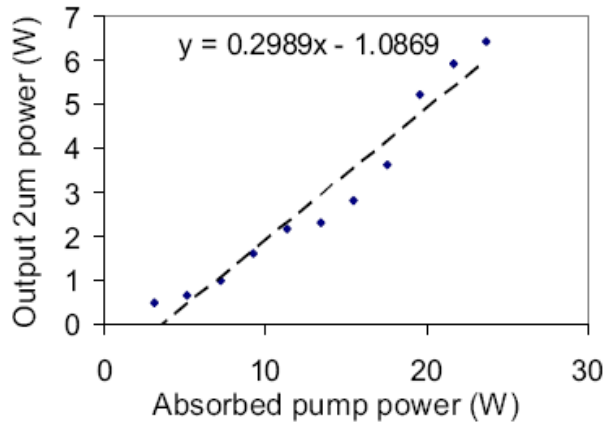


Figure 5-11: Output Performance of the Amplifier as a Function of Pump Power.

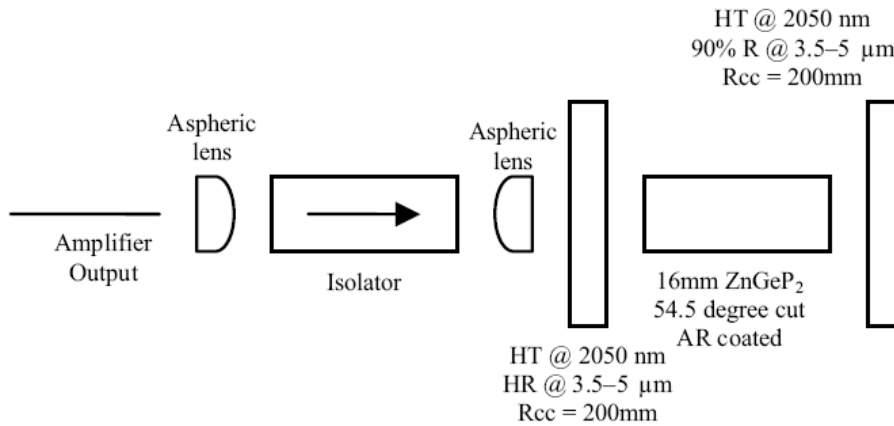


Figure 5-12: Zinc Germanium Phosphide Parametric Oscillator Pumped by Output of the Fiber Amplifier.

FIBER-PUMPED FREQUENCY CONVERSION DEVICES

In 2012, the Australian group presented a power-scalable, all-fiber, monolithic-pulsed source based on a thulium-doped fiber MOPA design (Figure 5-13) [18]. This source produced 200 μJ pulses 20 – 40 ns in duration at a repetition rate of up to 75 kHz, resulting in up to 12 W of linearly polarized output at 2.044 μm . This was used to pump a walk-off-compensated ZGP OPO which generated 3 W in the mid-IR, with a conversion efficiency of 25% (Figure 5-14).

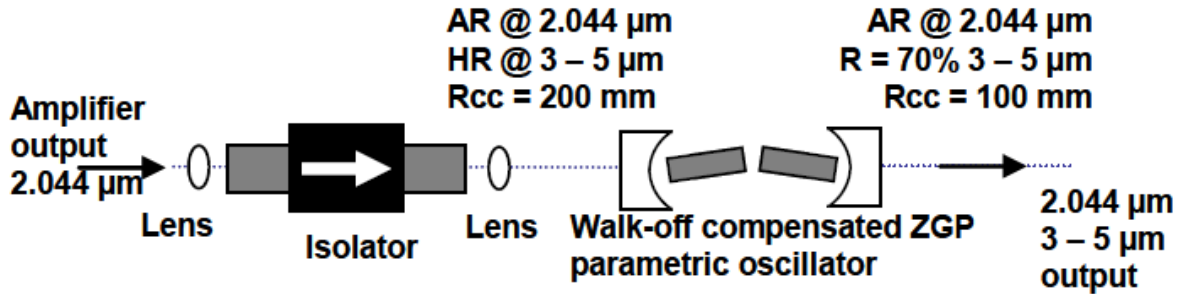


Figure 5-13: Schematic of Tm-Doped MOPA Pumping Dual-Crystal ZGP OPO.

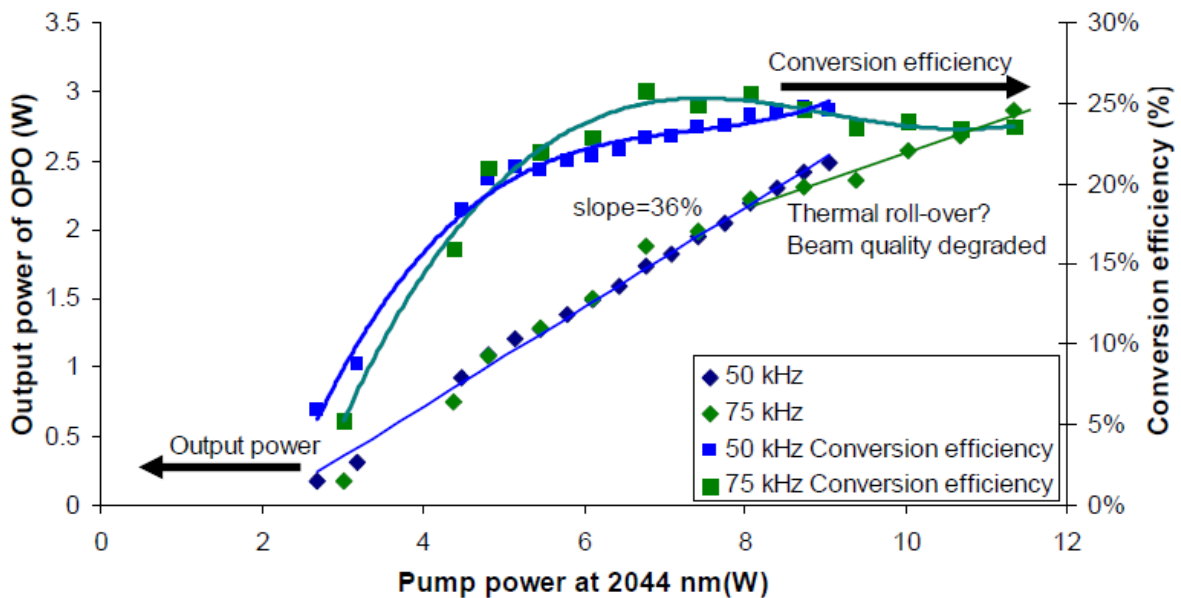


Figure 5-14: Output Power vs. Input Power and Conversion Efficiency of the OPO when Operating at 50 kHz and 75 kHz.

Pankaj Kadwani and co-workers from CREOL, University of Central Florida (USA) and Friedrich-Schiller-Universität (DEU) reported a Tm-fiber MOPA system using a power amplifier based on a Photonic Crystal Fiber (PCF), generating over 40 kW peak power in ~ 6.5 ns pulses as a tunable, narrow linewidth pump for mid-IR ZGP OPOs [19]. The initial experimental OPO set-up can be seen in Figure 5-15. The Q-switched oscillator is based on a Tm fiber pumped by a 35 W laser diode operating at 790 nm. Pulse energies of $> 200 \mu\text{J}$ were achieved at 20 kHz, and $> 400 \mu\text{J}$ at 1 kHz, with ~ 6.5 ns pulse duration. The spectral linewidth was < 1 nm FWHM. The output passed through an optical isolator and an extra-cavity EO pulse picker, before being focused by a 400 mm focusing lens to a $\sim 225 \mu\text{m}$ diameter waist in a ZGP crystal with dimensions of 4 mm x 5 mm x 12 mm cut at $\theta = 57.5^\circ$. The ZGP crystal was placed between two flat mirrors forming a doubly resonant OPO cavity. The input coupler was $> 99\%$ reflective and output

coupler ~ 50 % reflective over the 3 – 5 μm wavelength range, while both mirrors were highly transmissive at the pump wavelength. A longpass filter removed residual pump light. The use of PM fiber increased the overall efficiency compared with the first demonstration by Creeden et al. using an unpolarized pump beam.

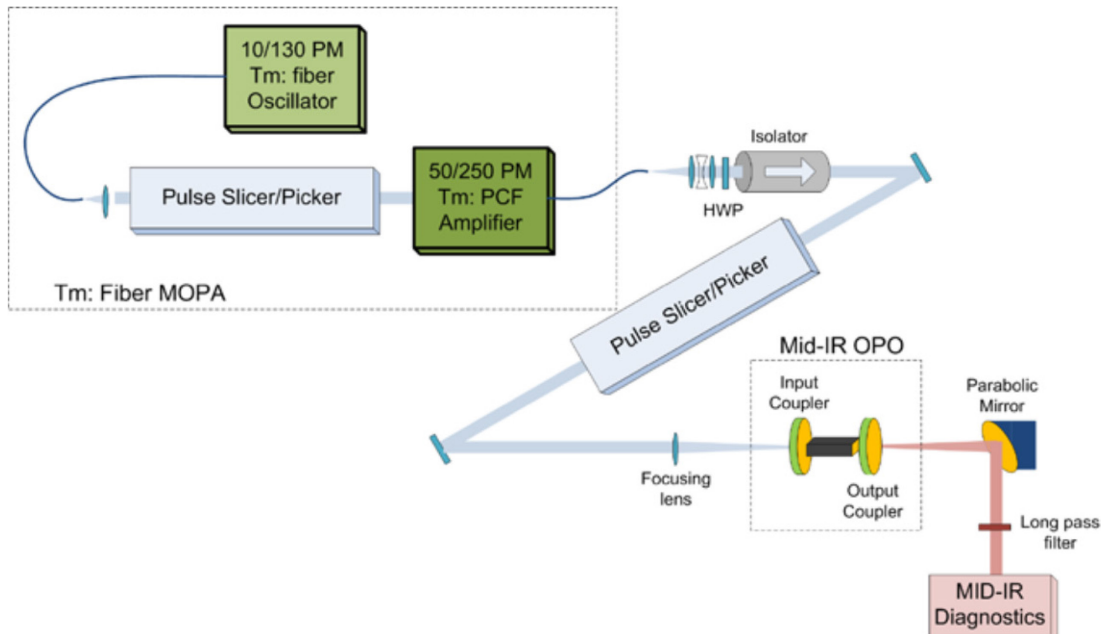


Figure 5-15: MOPA System Where a 10/130 SMF Fiber Oscillator Seeds a Flexible Tm:PCF Amplifier Through a Pulse Slicer. The output is passed through a pulse picker and focused into a ZGP OPO by a 400-mm lens. The output is then collimated by a parabolic mirror and sent through a mid-IR filter to beam diagnostics.

Figure 5-16 shows the output characteristics of this ZGP OPO for three different repetition rates. The maximum total mid-IR energy is ~ 24 μJ which corresponds to about ~ 2 kW peak power for the signal (~ 3.55 μm). At the Mid-Infrared Coherent Sources (MICS) conference held in Paris in October 2013, the CREOL group reported the generation of 28 kW peak power in a mid-IR ZGP OPO, pumped by a Tm: fiber MOPA system delivering ~ 8 ns pulses with ~ 120 kW of usable pump peak power at 1980 nm [20].

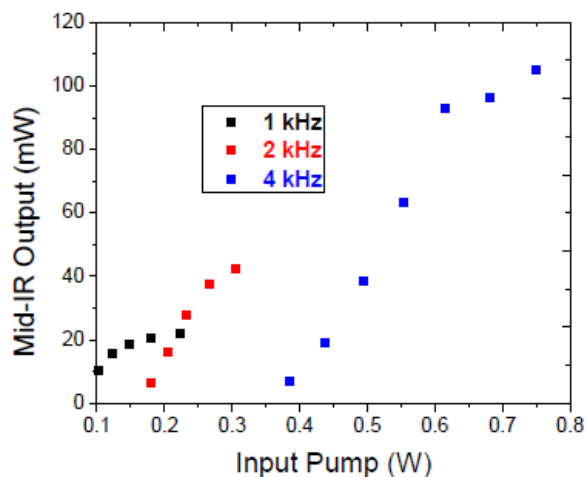


Figure 5-16: OPO Output for Several Repetition Rates, at ~ 6.8 ns Pulse Duration.

FIBER-PUMPED FREQUENCY CONVERSION DEVICES

5.2.3 OPGaAs

OPGaAs is a Quasi-Phase-Matched (QPM) non-linear crystal allowing for tight focusing, long interaction length and alignment insensitivity required for efficient conversion in a fiber-coupled device. It was the first material to demonstrate the potential of all epitaxial-grown QPM semiconductors and it is already achieving record output powers and efficiencies in the mid-IR. Its IR transparency is broader than that of PPLN and even ZGP. It also offers a higher non-linear coefficient, higher thermal conductivity, low losses when grown from the vapor phase, and is relatively insensitive to pump polarization, compared with other non-linear materials.

5.2.3.1 OPGaAs OPO Directly Pumped by a 2.09 μm Q-Switched Tm,Ho:silica Fiber Laser

The ISL group demonstrated an OPGaAs OPO directly pumped by a 2.09 μm Q-switched Tm,Ho:silica fiber laser [21],[22]. The experimental set-up is shown in Figure 5-17. The pulsed fiber laser is based on a Tm,Ho-doped double clad fiber (OFTC Sydney, Australia), Q-switched by a high diffraction efficiency (> 85%) TeO₂ Acousto-Optic Modulator (AOM) in an external cavity set-up [23]. A Volume Bragg Grating (VBG) was used to narrow the spectral line width emitted. Optical isolation was used between the fiber laser and the OPO cavity. The pump beam is split in two polarized beams by a Brewster plate, allowing separated optical isolation in two arms. The slightly multi-mode nature of the fiber used and the superposition of the two separated isolated beams led to a non-optimized beam in the non-linear crystal. The recombined pump beam was focused by a $f = 200$ mm lens to a ~ 200 μm spot inside the OPGaAs sample. Figure 5-18 plots the averaged powers curves for a plane-plane OPO cavity and plane-rcc 50-mm OPO cavity. The fiber laser was operated at a stable point of operation for repetition rates from 40 to 75 kHz. With a 2.09 μm Q-switched Tm,Ho:silica fiber laser pump source, up to 2.2 W of average output power was achieved at 40 kHz repetition rate, 1.9 W at 60 kHz and 1.1 W at 75 kHz with the plane-plane OPO-cavity. With the plano – 50 mm – radius-of-curvature OPO cavity, 1.88 W was achieved at 40 and 60 kHz, and 1.2 W at 50 and 75 kHz. Experiments were pump-power limited.

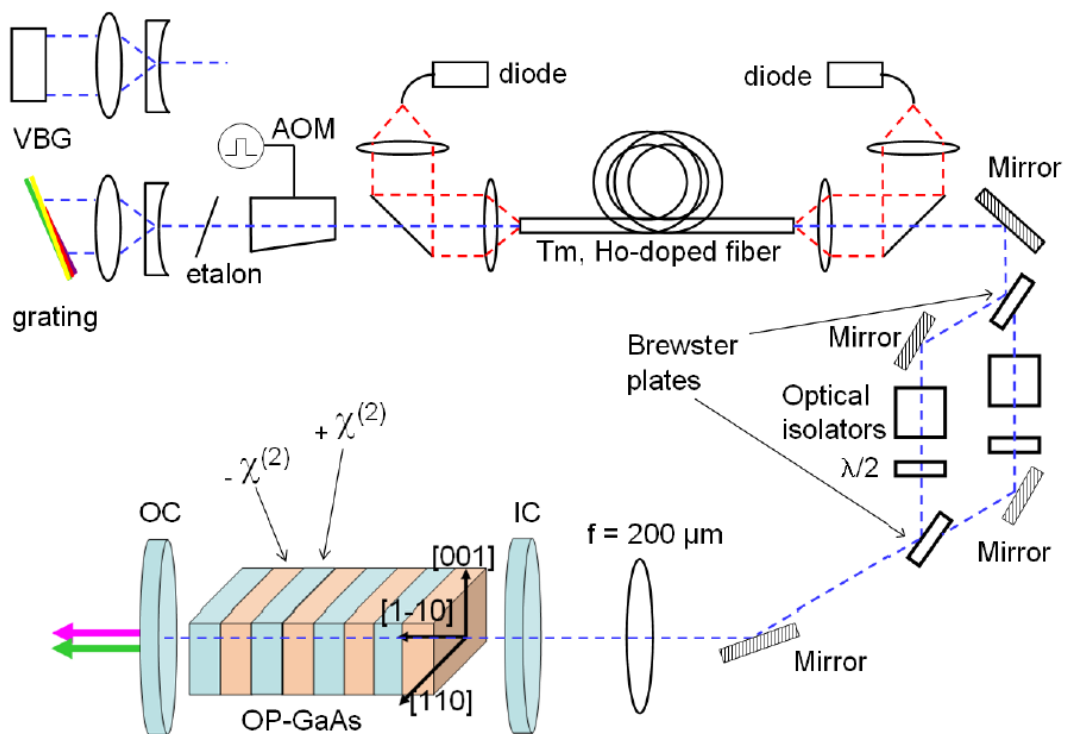


Figure 5-17: Experimental Set-Up for the OPGaAs OPO Pumped by a Tm,Ho-Doped Fiber.

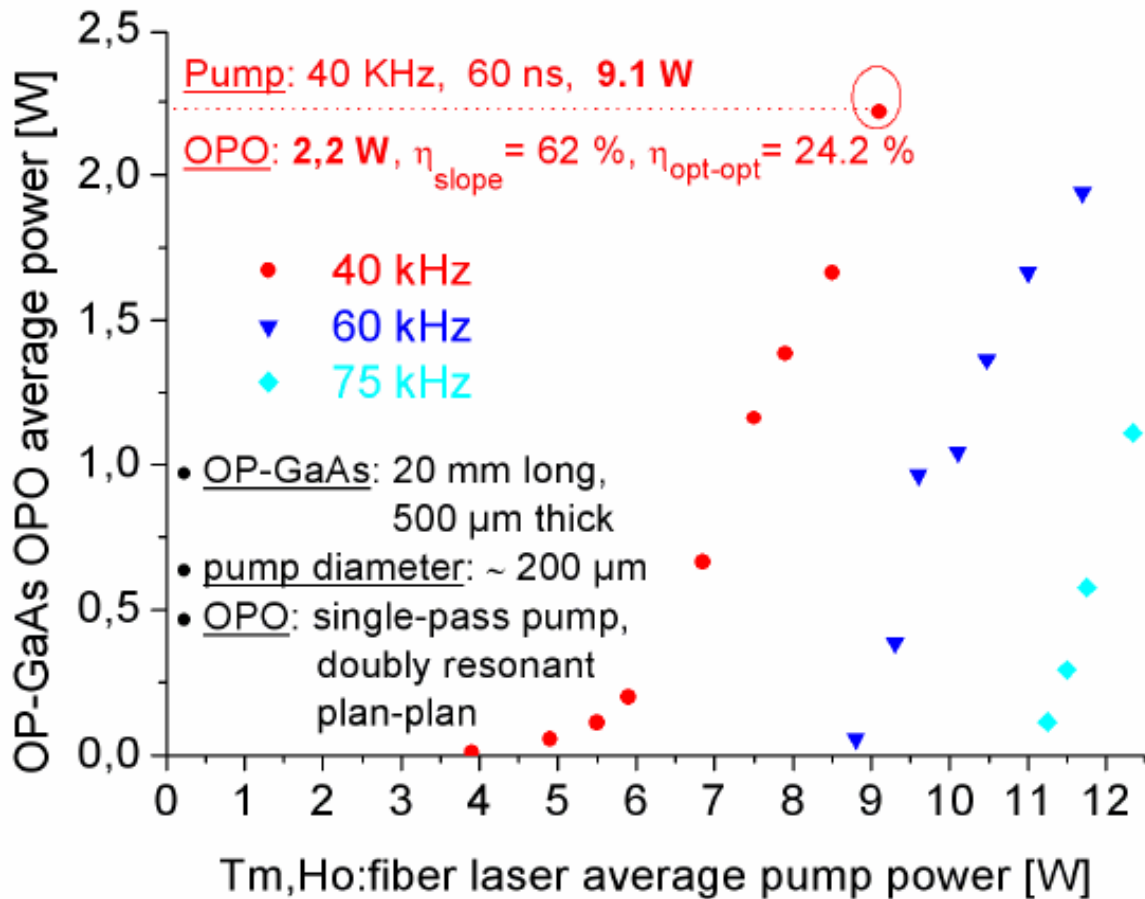


Figure 5-18: Output Average Power Performance of the Fiber Laser Pumped Plane-Plane OPGaAs OPO at 40, 62 and 75 kHz Repetition Rates.

The ISL group is currently working on a new pump set-up allowing for higher pump power and based on a monomode, polarization maintaining Tm, Ho-doped fiber to increase the overall conversion efficiency.

5.2.3.2 Mid-IR Conversion Efficiency from an OPGaAs Pumped by a 1.5 μm Erbium:Fiber Laser

5.2.3.2.1 Simulation

Contributors to this section: Pierre Mathieu⁹, Denis Vincent⁹, Francis Théberge⁹

Development of a multi-wavelength pump source emitting around 1550 nm is part of the concept put forward by DRDC-Valcartier to achieve the emission of radiation around 4 μm . One of the key concepts is to use the laser at 1535 – 1565 nm as an optical pump for OPO conversion by using the appropriate non-linear medium, here an Orientation-Patterned Gallium Arsenide (OPGaAs) crystal. For this section, we describe briefly the dual-wavelength Erbium fiber laser developed by Institut National d'Optique (INO), Canada, for a research project of the Defence R&D Canada. Experimental results for the difference frequency mixing in OPGaAs pumped by this laser cannot be presented because the OPGaAs crystal was not yet available when this report was written. However, simulation of the OPGaAs pumped by a multi-watt Er: fiber laser is presented using laser pump parameters very similar to the one acquired by DRDC-Valcartier.

⁹ DRDC Valcartier, 2459 route de la Bravoure, Québec (Québec) G3J 1X5, Canada.

FIBER-PUMPED FREQUENCY CONVERSION DEVICES

The Er: fiber laser acquired by DRDC-Valcartier emits an average output power of 18 W at 1535 nm and 1563 nm with modulation at the rate between pulsed and continuous wave regimes. This laser uses the MOPAW technology (Master Oscillator with Programmable Amplitude Wavefront) developed at INO and it is used to control the shape and repetition rate of the pulses. The repetition rate can be varied from 200 kHz to 1 MHz with a pulse width of 20 ns. The laser can also operate in a quasi-continuous regime at 100 MHz. The choice of wavelength (1535 nm or 1565 nm), repetition rate and pulse modulation can be varied at a rate greater than 3 kHz via TTL signals.

The simulations of the difference frequency generation using an OPGaAs crystal into an Optical Parametric Oscillator (OPO) pumped by such Er: fiber laser pulse have been done by using both SNLO and SiSyFos (software from G. Arisholm at Norwegian Defence Research Establishment). Because of the limitation of SNLO, for the first series of simulation presented in this section, we compare the calculations from SNLO and SiSyFos for the pump laser parameters with a Gaussian temporal profile and we neglect the two-photon absorption. In the second set of simulation, we use only the SiSyFos software with a high-order super-Gaussian temporal profile pump pulse (similar to the acquired dual-wavelength Er: fiber laser). For these simulations, we considered a single longitudinal mode for the pump which can underestimate the peak intensity and consequently the Two-Photon Absorption (TPA). Therefore, we considered three different values for the two-photon absorption, including one value being two-times larger than the TPA measured in [25]-[26].

First, for the comparison of the SNLO and SiSyFos simulations, we used a 1563 nm pump pulse with 20 ns Gaussian pulsewidth at FWHM and waist diameter of 165 μm centered into the OPGaAs crystal. The parameters of the OPGaAs for the simulation were a crystal length of 15 mm, a grating period around 28 μm maintained at 80 deg. C, a linear absorption of 0.03 cm^{-1} for the three wavelength involved (pump, signal and idler), and a non-linear coefficient $d_{14} = 94 \text{ pm/V}$. The parameters of the OPO cavity used for the simulations were a singly resonant double concave cavity using two mirrors having a radius of curvature of 250 mm. The gap between the ends of the OPGaAs crystal and the mirror surfaces were 7.5 mm. As shown in Figure 5-19, the reflectivity of the first mirror was 0%, 99% and 99% for the pump, signal and idler, respectively. The reflectivity of the second mirror (output coupler) was 99% and 0% for the pump and idler, respectively. For the output coupler, the reflectivity for the signal was adjusted to optimize the idler output power.

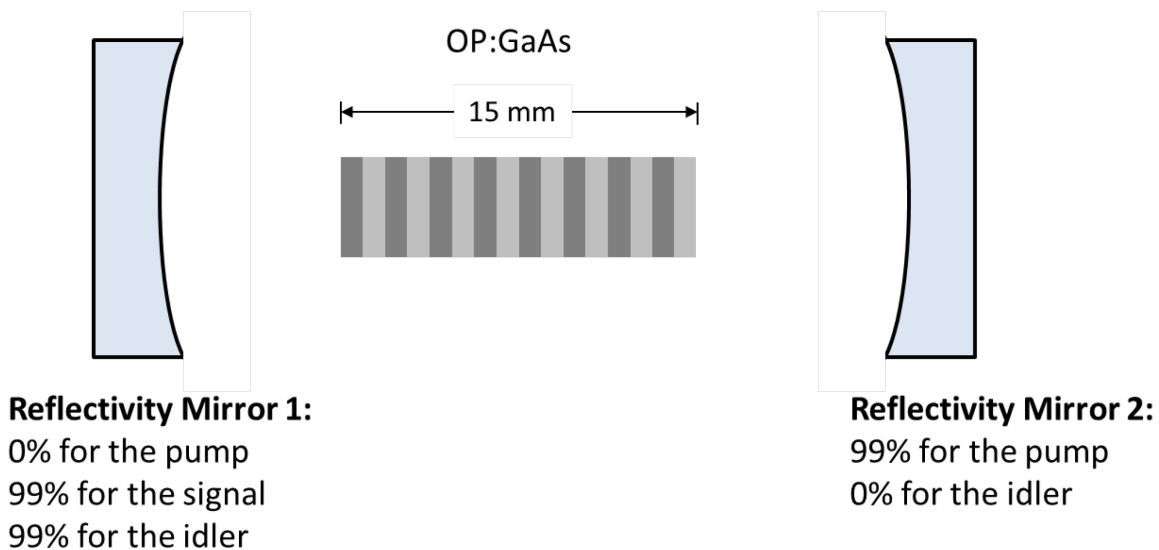


Figure 5-19: Schematic Diagram of the OPGaAs Optical Parametric Oscillator Used for the Simulations.

Table 5-1 presents the simulated output energies of the generated Idler (I) and Signal (S) for different 1563 nm pump pulse energies (P) and for the optimum signal reflectivity of the output coupler (RS,OC), for both the SNLO and the SiSyFos software. When comparing the SNLO and SiSyFos simulation results for pump energy far from the threshold energy for oscillation, we observe a fair agreement between the results of these two simulations for both the optimal signal reflectivity of the output coupler and the parametric conversion efficiency.

Table 5-1: Simulated Optimum Reflectivity of the Output Coupler and Corresponding Conversion Efficiency for Different Pump Pulse Energy.

| Pump Energy μJ | $R_{s,oc}$ | | Ratio I/P | | Ratio (I+S)/P | |
|------------------------------|------------|---------|-----------|---------|---------------|---------|
| | % | | % | | % | |
| | SNLO | SiSyFos | SNLO | SiSyFos | SNLO | SiSyFos |
| 12 | 85 | 95 | 23 | 5 | 46 | 8 |
| 24 | 60 | 80 | 26 | 19 | 62 | 41 |
| 48 | 60 | 60 | 28 | 24 | 67 | 56 |

For the second step of these simulations, we simulate the optical parametric generation with an OPGaAs OPO similar to the one presented in Figure 5-19, but this time the crystal length was fixed at 10 mm. Also we use only the SiSyFos software with a 12-order super-Gaussian pump laser pulse of 20 ns pulsewidth (FWHM), which is very similar to the top-hat pulsewidth from the acquired Er: fiber pump laser. For these simulations, we will compare also different values of the two-photon parameter of the GaAs at 1563 nm (β_{1563nm}). From values available in open literature, the GaAs two-photon parameter corresponds to $\beta_{1563nm} = 10 \text{ cm/GW}$ [23],[24]. In Figure 5-20, we compare the parametric conversion efficiency for different pump energy and different value of β_{1563nm} corresponding respectively to 0 cm/GW, 10 cm/GW and 20 cm/GW. From the results presented in Figure 5-20, we observe that a variation of β_{1563nm} and/or the peak intensity of pump pulse do not affect too severely the pump absorption and the parametric conversion efficiency.

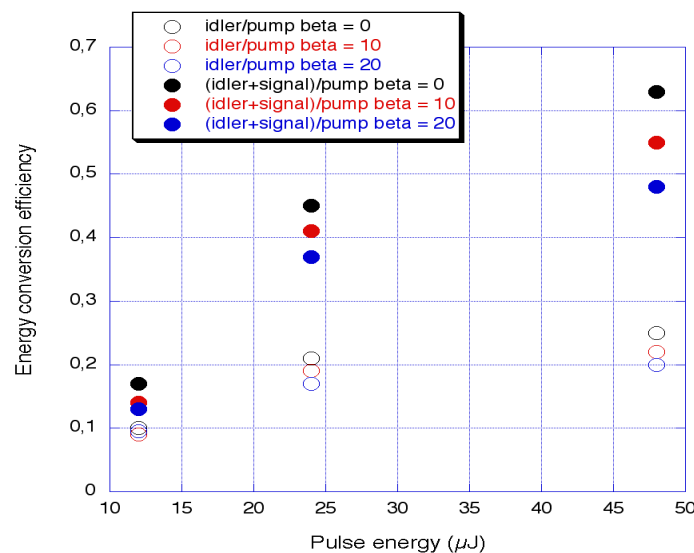


Figure 5-20: Ratio of the Parametric Energy Over the Pump Energy as a Function of the Pump Energy for Different Values of the GaAs Two-Photon Absorption (Beta).

FIBER-PUMPED FREQUENCY CONVERSION DEVICES

Figure 5-21 presents the temporal evolution of the pump, signal and idler pulses in the OPGaAs OPO for a neglected two-photon absorption ($\beta_{1563\text{nm}} = 0$ in Figure 5-21(a) and a two-photon parameter of $\beta_{1563\text{nm}} = 10$ cm/GW (Figure 5-21(b)). For these two cases, the optimum reflectivity of the signal for the output coupler was also calculated and corresponds to 40% and 35% for Figure 5-21(a) and Figure 5-21(b), respectively. By comparing these two results, we observe again that two-photon absorption does not have too severe an impact on the parametric conversion, at least for the range of pump power/energy used for these simulations.

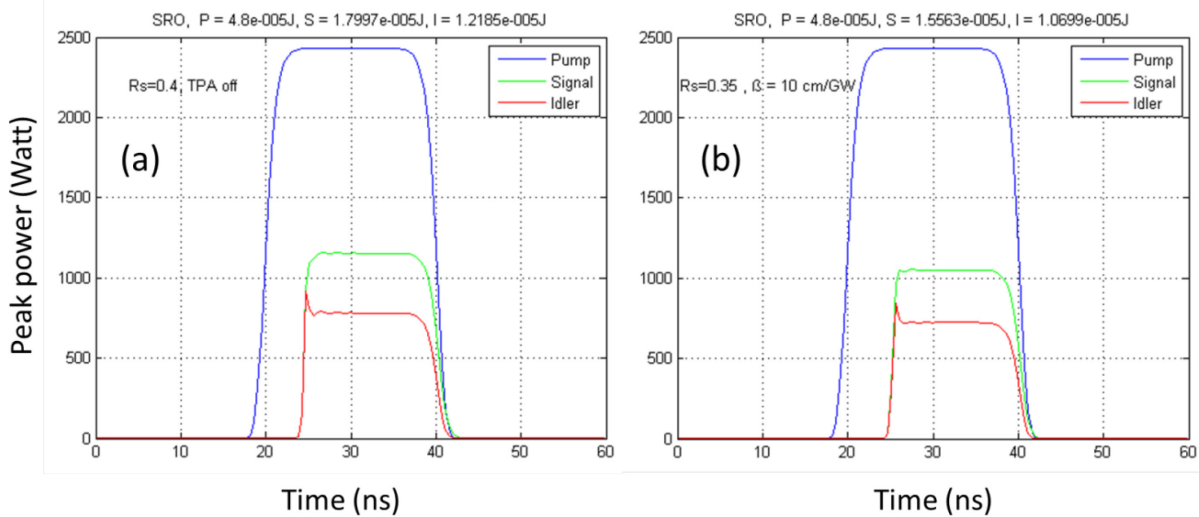


Figure 5-21: Temporal Evolution of the Pump, Signal and Idler Laser Pulses for a Two-Photon Absorption Parameter of (a) $\beta_{1563\text{nm}} = 0$ cm/GW, and (b) $\beta_{1563\text{nm}} = 10$ cm/GW.

5.2.3.2.2 Growth of OPGaAs for 1.5 μm Pumping

Contributor to this section: Rita D. Peterson¹⁰

Producing mid-infrared (3 – 5 μm) output using a 1.5 μm pump in OPGaAs requires a period around 27 – 28 μm . Air Force Research Laboratory (AFRL) had on-hand two template segments with periods in the 27 – 29 μm range, suitable for this interaction. A growth run was made on one of these in April 2011, in the HVPE reactor then located at Hanscom Air Force Base, using a process documented in the literature [25]. This was one of the last growth experiments performed before the laboratory was relocated to Ohio, USA.

The growth run was unfortunately unsuccessful. The domain structure was completely overgrown within the first 100 μm of growth. This was not unexpected, since most material grown in this process to date has had periods larger than 50 μm , and previous thick growth attempts of domains < 20 μm have produced poor results. After the laboratory is back in service in its new location, the remaining template piece will be used to test modifications to the growth conditions. If interest remains in 1.5 μm pumping of OPGaAs, a new template will be fabricated with the required periods, for use in future growth experiments. Understanding how to adjust growth conditions to produce smaller periods is of general interest as the repertoire of OPGaAs-based devices continues to expand.

As part of a consolidation of AFRL facilities, the HVPE growth laboratory was relocated from Hanscom Air Force Base in Massachusetts to Wright-Patterson Air Force Base in Ohio in the summer of 2011. The last growth experiments at Hanscom AFB were completed in May 2011. The growth laboratory includes three

¹⁰ Air Force Research Laboratory, AFRL/RYPJW Bldg 620, 2241 Avionics Circle, Wright-Patterson AFB, OH 45433, United States.

HVPE reactors, for growth of GaAs, GaP, and nitrides respectively; all of which received new components and upgrades when reassembled in the new location. The OPGaAs reactor was the first to return to service, beginning with short calibration runs to validate growth conditions. Long growth runs to produce thick samples for device experiments resumed in June 2013. The material quality of these samples is comparable to that of samples grown prior to the lab relocation. A representative cross-section showing the domain structure is shown in Figure 5-22 where the period is $116\ \mu\text{m}$.

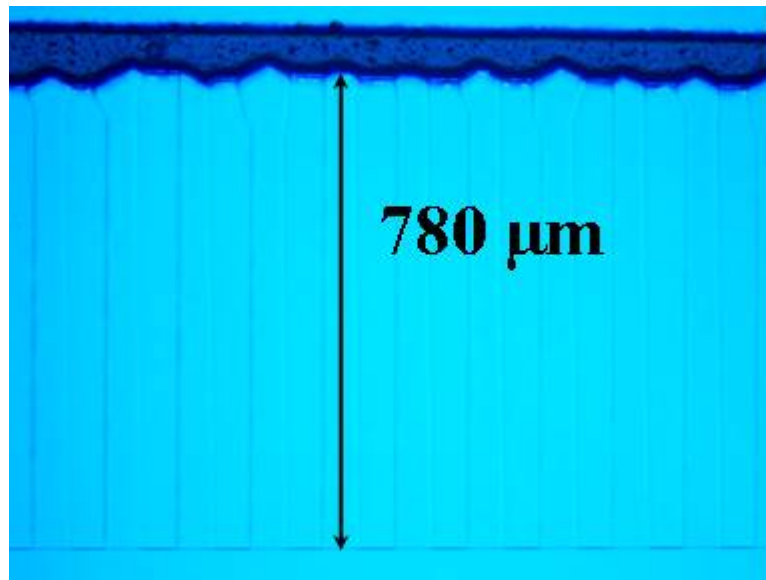


Figure 5-22: Cross-Section of Recent Thick GaAs Growth.

5.3 CONCLUSION AND OUTLOOK

Efficient pumping of OPGaAs and ZGP depends upon pump sources emitting at wavelengths higher than $1.73\ \mu\text{m}$ and $2\ \mu\text{m}$ respectively, to avoid absorption losses while minimizing quantum defect. Analysis of the state-of-the-art indicates that more progress is needed on pump fibers and optical components in this wavelength region, to support the eventual goal of eliminating free-space coupling in future mid-IR fiber sources, allowing systems that are completely optically confined.

The experimental demonstration of mid-infrared ($3 - 5\ \mu\text{m}$) output using a $1.5\ \mu\text{m}$ pump in OPGaAs has to be performed to confirm the DRDC simulation results that predict reasonably efficient output, despite the reported severe two-photon absorption at wavelengths shorter than $1.7\ \mu\text{m}$.

Continued progress in QPM semiconductors for mid-IR frequency conversion has been reported [26],[27]. This includes the introduction of Orientation-Patterned Gallium Phosphide (OPGaP) as an alternative to OPGaAs having negligible two-photon absorption in the convenient pumping range from $1\ \mu\text{m}$ to $1.7\ \mu\text{m}$ where efficient fiber lasers are readily available. OPGaP material up to $350\ \mu\text{m}$ thick has been grown, but device experiments have yet to be reported.

5.4 REFERENCES

- [1] Suter, J.D., Bernacki, B.E. and Phillips, M.C. Angle-resolved scattering spectroscopy of explosives using an external cavity quantum cascade laser, Proc. SPIE 8268, 82681O (2012).

FIBER-PUMPED FREQUENCY CONVERSION DEVICES

- [2] Neese, C.F. Infrared/terahertz double resonance for chemical remote sensing: signatures and performance predictions, Proc. SPIE 7671, 76710F (2010).
- [3] Fuchs, F., Hinkov, B., Hugger, S., Kaster, J.M., Aidam, R., Bronner, W., Köhler, K., Yang, Q., Rademacher, S., Degreif, K., Schnürer, F. and Schweikert, W. Imaging stand-off detection of explosives using tunable mid-IR quantum cascade lasers, Proc. SPIE 7608, 760809 (2010).
- [4] Seddon, A.B., Tang, Z., Furniss, D., Sujecki, S. and Benson, T.M. Progress in rare-earth-doped mid-infrared fiber lasers, Opt. Expr. 18(25), 26704-26719 (2010).
- [5] <http://www.wsof2013.org/isla-integrated-disruptive-components-2-%CE%BCm-fibre-lasers>.
- [6] www.inradoptics.com White Paper (2013).
- [7] Bonetti, Y. and Faist, J. Quantum cascade lasers: Entering the mid-infrared, Nature Photonics 3, 32-34 (2009).
- [8] Matsuoka, N., Yamaguchi, S., Nanri, K., Fujioka, T., Richter, D. and Tittel, F. Yb fiber laser pumped mid-IR source based on difference frequency generation and its application to ammonia detection, Jpn. J. Appl. Phys., 40, 625-628 (2001).
- [9] Jiang, J., Chang, J.-H., Feng, S.-J., Mao, Q.-H. and Liu, W.-Q. Mid-IR dual-wavelength difference frequency generation using fiber lasers as pump and signal light sources, Chin. Phys. Lett. 26(12), 124214 (2009).
- [10] Winters, D.G., Schlup, P. and Bartels, R.A. Subpicosecond fiber-based soliton-tuned mid-infrared source in the 9.7-14.9 μm wavelength region, Opt. Lett. 35(13), 2179-2181 (2010).
- [11] Chang, J., Mao, Q., Feng, S., Gao, X. and Xu, C. Widely tunable mid-IR difference-frequency generation based on fiber lasers, Opt. Lett. 35(20), 3486-3488 (2010).
- [12] Neely, T.W., Johnson, T.A. and Diddams, S.A. High-power broadband laser source tunable from 3.0 μm to 4.4 μm based on a femtosecond Yb: fiber oscillator, Opt. Lett. 36(20), 4020-4022 (2011).
- [13] Salhany, J. and Burgoyne, B. FIBER LASERS: Programmability comes to fiber lasers, Laser Focus World 48(3) (2010).
- [14] Creeden, D., Ketteridge, P.A., Budni, P., Zawilski, K., Schunemann, P.G., Pollak, T.M. and Chicklis, E.P. Multi-Watt Mid-IR Fiber-Pumped OPO, Conference on Lasers and Electro-Optics CLEO 2008, paper CTuII2 (2008).
- [15] Creeden, D., Ketteridge, P.A., Budni, P.A., Setzler, S.D., Young, Y.E., McCarthy, J.C., Zawilski, K. and Schunemann, P.G. Mid-infrared ZnGeP₂ parametric oscillator directly pumped by a pulsed 2 μm Tm-doped fiber laser, Opt. Lett. 33(4), 315-318 (2008).
- [16] <http://ftp.rta.nato.int/public//PubFullText/RTO/MP/RTO-MP-SET-171///%24MP-SET-171-T.pdf>.
- [17] Simakov, N., Hemming, A., Davidson, A., Carmody, N., Bennetts, S., Davies, P. and Haub, J. Power Scalable 2 μm Source for Parametric Generation of Mid-infrared Radiation in ZnGeP₂, 35th Australian Conference on Optical Fibre Technology (ACOFT) (2010).
- [18] Simakov, N., Davidson, A., Hemming, A., Bennetts, S., Hughes, M., Carmody, N., Davies, P. and Haub, J. Mid-Infrared Generation in ZnGeP₂ Pumped by a Monolithic, Power Scalable 2 μm Source, Proc. of SPIE Vol. 8237, 82373K-1 (2012).

- [19] Kadwani, P., Gebhardt, M., Gaida, C., Shah, L. and Richardson, M. A High Peak Power, Nanosecond Tm: fiber MOPA System for Mid-IR OPO Pumping, Conference on Lasers and Electro-Optics CLEO 2013, Paper JW2A.29 (2013).
- [20] Gebhardt, M., Gaida, C., Kadwani, P., Sincore, A., Gehlich, N., Shah, L. and Richardson, M. Nanosecond Tm: fiber MOPA System for High Peak Power Mid-IR Generation in a ZGP OPO, Mid-Infrared Coherent Sources (MICS) – Paris, Paper MW3B.2 (2013).
- [21] Kieleck, C., Hildenbrand, A., Eichhorn, M., Faye, D., Lallier, E., Gérard, B. and Jackson, S.D. OP-GaAs OPO Pumped by 2 μ m Q-switched Lasers: Tm:Ho:Silica Fiber Laser and Ho:YAG Laser, Proc. SPIE 7836, 783607 (2010).
- [22] Eichhorn, M. and Jackson, S.D. High-pulse-energy, actively Q-switched Tm³⁺, Ho³⁺-codoped silica 2 μ m fiber laser, Optics Letter, 33 (10), 1044-1046 (2008).
- [23] Tani, M., Lee, K.-S. and Zhang, X.-C. Detection of terahertz radiation with low-temperature-grown GaAs-based photoconductive antenna using 1.55 μ m probe, Appl. Phys. Lett. 77, p. 1396 (2000).
- [24] Hurlbut, W.C., Lee, Y.-S., Vodopyanov, K.L., Kuo, P.S. and Fejer, M.M. Multiphoton absorption and nonlinear refraction of GaAs in the mid-infrared, Opt. Lett. 32(6), 668-670 (2007).
- [25] Bliss, D.F., Lynch, C., Weyburne, D., O’Hearn, K. and Bailey, J.S. Epitaxial growth of thick GaAs on orientation-patterned wafers for nonlinear optical applications, Journal of Crystal Growth, Vol. 287 673-678 (2006).
- [26] Schunemann, P.G. and Setzler, S.D. Future directions in quasi-phasematched semiconductors for midinfrared lasers, Proc. of SPIE Vol. 7917, 791750 (2011).
- [27] Tassev, V., Snure, M., Peterson, R., Schepler, K.L., Bedford, R., Mann, M., Vangala, S., Goodhue, W., Lin, A., Harris, J., Fejer, M. and Schuneman, P. Progress in orientation-patterned GaP for next-generation nonlinear optical devices, Proc. of SPIE Vol. 8604, 8604-31 (2013).

